RSC Advances

ROYAL SOCIETY OF CHEMISTRY

www.rsc.org/advances

Cite this: DOI: 10.1039/c0xx00000x

www.rsc.org/xxxxxx

PAPER

N-doped, S-doped TiO_2 nanocatalysts: Synthesis, Characterization and Photocatalytic Activity in Presence of Sunlight

P.V.R.K. Ramacharyulu[a]*, Dipak Bapurao Nimbalkar[a], J. Praveen Kumar[b], G.K. Prasad[b]* and Shyue-Chu Ke[a]*

Received (in XXX, XXX) Xth XXXXXXXXX 20XX, Accepted Xth XXXXXXXXX 20XX
DOI: 10.1039/b000000x

N doped and S doped nanoTiO_2 catalysts were synthesized by sol-gel followed by hydrothermal treatment at low temperature and tested for catalytic activity by natural sunlight photocatalytic degradation of the toxic chemical warfare agent. It is observed that sulfate groups were anchored on the surface of titania upon doping, and also creates active surface oxygen vacancies, both which are responsible for sunlight absorption and the promotion of electrons to the conduction band. Formation of superoxide radical ($O_2^{\bullet-}$) and hydroxyl radicals which may be mainly responsible for photodegradation of sulfur mustard under sunlight.

1. Introduction

Recently there has been growing interest on visible light active photocatalyts and their applications in environmental remediation and also for the preparation of organic compounds that are difficult to prepare by alternative methods. The visible light active photocatalyst effectively utilizes sunlight and promises widespread applications related to degradation of toxic chemicals with low energy consumption. TiO_2, an economical, nontoxic, and highly effective photocatalyst, has been widely used for degradation of toxic chemicals in light irradiation. However, TiO_2, because of its large band gap value 3.2 eV, can only be activated by 3-4 % of UV light fraction of the whole radiant sunlight. In order to use sunlight effectively, TiO_2 needs to be modified further [1]. Doping of TiO_2 with metal cations or main group elements was observed to induce extension of the absorption spectrum into visible light region [2-3]. Although transition metals exhibited the desired red shift of absorption maxima, many of them were also found to act as recombination centers [4].

It was reported that narrowing of band gap of TiO_2 could be achieved by using non-metal species instead of metal ions. Sulfur or nitrogen substitutional doping on TiO_2 was found to be effective for reducing the band gap values. The S or N atoms occupy the vacant sites of either titanium ion or oxygen in the titania lattice. Subsequently, the mixing of S3p states with valance band was found to contribute to band gap narrowing [5]. The large electronegativity differences between S, N, and O atoms were found to assist the formation of $TiO_{1-x}S_x$ or $TiO_{1-x}N_x$ structure which led to the shift of threshold wave length to visible light region [6-7]. Asahi *et al.* reported theoretical calculations of the band structure of nitrogen doped TiO_2 and studied photocatalytic degradation of acetaldehyde and methylene blue with irradiation of visible light [8]. They found that nitrogen atoms substituted the lattice oxygen sites and narrowed the band gap due to mixing of N2p and O2p states. Similarly, several other groups investigated the photocatalytic properties of nitrogen doped TiO_2 powders and thin films prepared by different methods [9-13]. Hashmito *et al.* reported the photocatalytic decomposition of 2- propanol. They found that decomposition of propanol decreased with increased N dopant content on TiO_2 when irradiated with visible light. This was attributed to an increase of oxygen vacancies, which promoted the recombination of electrons and holes with increased dopant concentration [6].

Umebayashi *et al.* synthesized S doped TiO_2, and used it for the studies on photocatalytic degradation of methylene blue under visible light irradiation [14-16]. They observed that sulphur was doped as an anion and replaced the lattice oxygen in TiO_2. On the other hand, Ohno *et al.* found that S atoms were incorporated as cations and replaced Ti ions in the S doped TiO_2 [17-19]. It is interesting that S atoms unlike other non metal dopants could exist in more than one oxidation state such as S^{2-}, S^{4+} or S^{6+} on TiO_2 depending on the conditions of synthesis or the type of sulfur precursors. Irrespective of sulfur oxidation state, the photocatalytic activity was found to be enhanced [18,20] .

Sulfur mustard ($C_4H_8SCl_2$, 2, 2'-dichloro diethyl sulfide, HD) is a vesicant, acts as a blister agent, alkylates DNA, and causes fatality to cells. Degradation of HD is a difficult process from the mechanism point of view [21]. Its photochemical decomposition in the presence of visible light suggests the possibility of the use of sunlight for degrading HD.

Recently, Prasad and co-workers have studied photocatalytic degradation of sulfur mustard using various catalysts like TiO_2, ZnO, MnO_2, V-TiO_2 [22(a-d)]. Each has its own disadvantages TiO_2 is visible inactive, it absorbs only UVA light in solar spectrum. ZnO absorbs some of the visible light but it takes more time for degradation. V-TiO_2 absorbs both UVA & visible light in solar spectrum but metal ions can act as recombination centres. However, Cojocaru *et al.* studied photocatalytic degradation of

CWA like Soman, VX, and Yperite on activated carbon supported with N doped and undoped TiO_2 of large particle size [23]. However, there are no reports available in literature on photocatalytic degradation of HD using S or N doped nano TiO_2 in the presence of sunlight. The present paper reports the synthesis of N doped TiO_2 (NT), S doped TiO_2 (ST) nanocatalysts by sol–gel method followed by hydrothermal treatment. This synthesis is eco-friendly as use of toxic precursors are avoided. The synthesized materials were characterized by using X-ray diffraction (XRD), Transmission electron microscopy (TEM), X-ray photoelectron spectroscopy (XPS), Nitrogen adsorption (BET), UV-vis absorbance spectroscopy, and Electron paramagnetic resonance spectroscopy (EPR) techniques. The photocatalytic degradation reactions of HD were studied in sunlight using gas chromatography (GC) and the resulting products were analysed using gas chromatography mass spectrometry (GC-MS). The obtained data on doped materials was compared with that of undoped (HT) and commercial TiO_2 (CT) nanocatalysts of anatase phase.

2. Results and discussions

2.1. Characterization of the ST, NT, HT nanocatalysts

Fig.1 shows the XRD patterns of ST, NT, and HT nanocatalysts. XRD patterns of all the nanocatalysts exhibit peaks at 25.2˚, 37.8˚, 48.0˚, 53.8˚, and 62.7˚ 2θ values which are characteristics of (1 0 1), (0 0 4), (2 0 0), (1 0 5), and (2 1 5) indices. The data confirmed the formation of ST, HT, and NT nanocatalysts with anatase phase (JCPDS 21-1272). CT nanocatalyst also exhibited anatase phase and the respective XRD data was already reported .

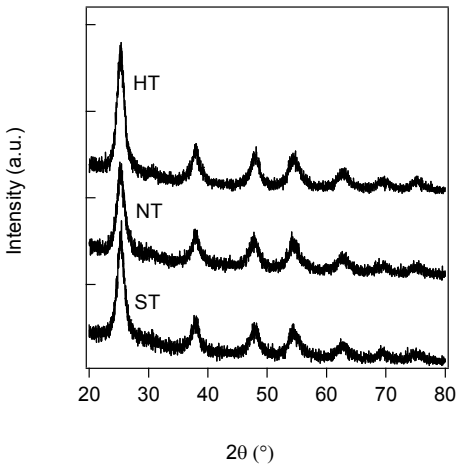

Fig. 1. XRD patterns of NT, ST, and HT nanocatalysts.

The crystallite sizes of synthesized nanocatalyst materials were calculated by Scherrer equation. Crystallite size of NT and HT nanocatalysts varied in between 6 to 10 nm. ST nanocatalyst showed a crystallite size of 4.8 nm. CT nanocatalyst showed crystallite size of 35 nm. XRD data shows similar peak patterns for ST, HT, and NT nanocatalysts. The S substituted for Ti^{4+} hinders the growth of TiO_2, therefore, the particle size of S-doped TiO_2 photocatalysts get smaller with the increasing sulfur doping.

TEM images of HT, ST, and NT nanocatalysts are presented in Fig. 2(a-c). TEM images indicate the particles of spherical shape that have been embedded in the agglomerates with sizes varying around 4.8 to 10 nm.

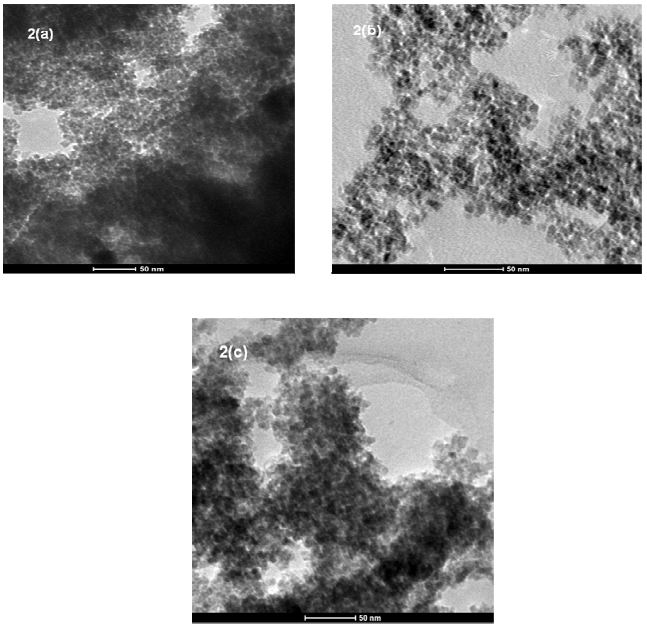

Fig.2 TEM images of (a) NT, (b) ST, and (c) HT nanocatalysts

Fig. 2

XPS spectra of ST nanocatalyst are shown in Fig.3(a). ST nanocatalyst shows a peak at 167 eV (S2p) depicting the presence of S^{4+} ion in its bulk. In addition to this, a shoulder peak at 168 eV (S2p) and a broad peak at 169 eV(S2p) indicate the presence of S^{6+} ion in the same and the data is consistent with previously reported data [18]. G.Yang *et al.* [24] demonstrated that there are two possible coordination models between SO_4^{2-} and TiO_2 as shown in *SI*. The formation of cationic S-doped TiO_2 could create a charge imbalance in the lattice of catalyst, and the extra positive charge is probably neutralized by the hydroxide ions.

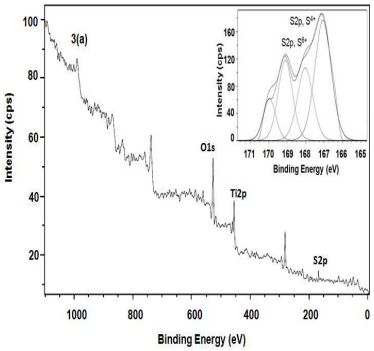

Fig.3(a) XPS spectra of ST (S-TiO_2)

XPS spectra of NT nanocatalyst are shown in Fig.3(b). NT nanocatalyst shows peaks at 398.3 (N1s), 399.7(N1s), and 401.3 eV(N1s) indicating the presence of O-Ti-N, N-O-Ti, and O-N-Ti-O structures in the bulk of same. It also shows peaks at 459.6 (Ti

$2p_{3/2}$), 464.9 (Ti $2p_{1/2}$), 531,532 eV (O1s), 284.6 eV (C1s) in the same (Fig.3(b)) and the data is consistent with previously reported data [8-9] . Where, HT nanocatalyst shows peaks 459.6, 464.9, 531, 532, 284.6 eV depicting $Ti2p_{3/2}$, Ti $2p_{1/2}$, O1s, C1s respectively [17-19]. The unmarked peaks in the spectra belong to Ti 2s, OKLL & Ti LMM respectively as reported in the literature.

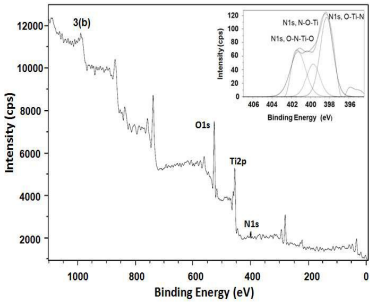

Fig.3(b). XPS spectra of NT (N-TiO_2)

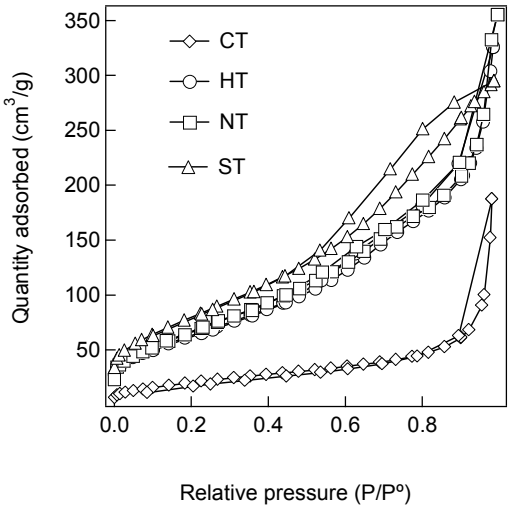

Fig. 4. Nitrogen adsorption isotherms of HT, ST, NT, and CT nanocatalysts.

Fig. 4 shows the nitrogen adsorption data of HT, ST, NT and CT nanocatalysts. All the nanocatalysts exhibit type IV adsorption isotherm typical of mesoporous materials with H3 type hysteresis. Isotherms also indicate the presence of slit type of pores formed due to aggregation of TiO_2 nanocatalysts either doped or undoped. When compared to HT (230 m^2/g), ST nanocatalyst exhibited slightly greater surface area (290 m^2/g) which can be ascribed to the presence of relatively more number of mesopores in ST nanocatalyst. S atom was found to have controlled the nucleation and growth of titania particles and facilitated the formation of some new mesopores which increased the surface area and mesopore volume and the same can be seen in Table 1 and Fig.4. Compared with undoped TiO_2, the particle size of the S-doped TiO_2 samples is much smaller, resulting in larger specific surface area. Small particle size can shorten the route for an electron migration from the interior of TiO_2 to surface, which can reduce the recombination of h^+ and e^-. Moreover, the larger the surface area, the more SO_4^{2-} it has. The SO_4^{2-} adsorbed on the surface of TiO_2 can trap photo-induced electrons (e^-), improving the quantum yield.

Type of nanocatalyst	BET Surface area (m^2/g)	Total pore volume (mL/g)	Meso pore volume (mL/g)
HT	230.4	0.50	0.07
ST	290.3	0.54	0.09
NT	243.3	0.54	0.08
CT	75.3	0.29	0.09

Table 1 Nitrogen adsorption data of HT, ST, NT, and CT nanocatalysts.

Fig. 5 shows the UV-vis spectra of the undoped, N-doped and S-doped TiO_2 powders. Very minute shifts of the absorbance shoulder from 400 nm to the visible light region are observed for the N and S-doped TiO_2. These results reveal that the nitrogen and sulfur dopants are on the surface of TiO_2 but not in the lattice of TiO_2. It might have happened due to formation of N^- atoms could have occupied interstitial sites in oxygen vacancies in N-TiO_2. In S-TiO_2 either S^{4+} or S^{6+} ions (SO_4^{2-}) could have anchored on TiO_2 . To understand the dopant localised state, the samples were annealed at 450 °C in Ar atmosphere, noticable shifts in the visible region were observed (*SI*). Dopants exists as localised states above the valence band thus altering its crystal and electronic structures.

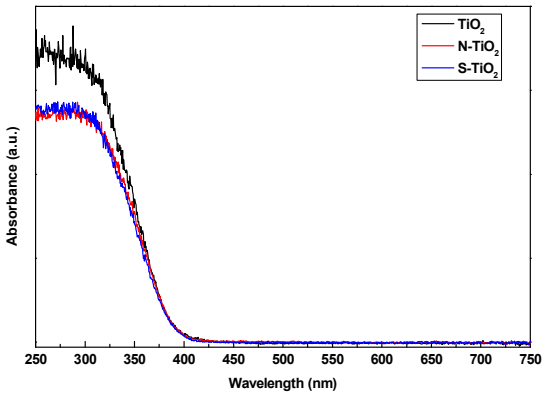

Fig.5. UV-vis absorbance of TiO_2, N-TiO_2 and S-TiO_2 nanocatalysts.

Electron paramagnetic resonance spectra were recorded under full-light illumination at 77K. EPR signals assigned photogenerated electrons trapped in anatase lattice Ti^{3+} ($g_\perp$=1.990 and $g_\parallel$=1.960) and hole on the anatase surface $O^{\bullet-}$ (g_1=2.016, g_2=2.012 and g_3= 2.003) can be seen in Fig.6. Excited electrons get trapped by conduction band defect site to produce Ti^{3+} signal and the remained hole in the valence band which can react with O_2, H_2O and hydroxide ion to from hydroxyl radical [25].

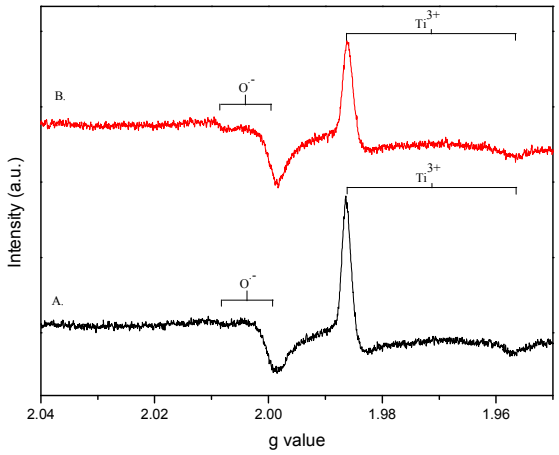

Fig.6. EPR spectra of (A) N-TiO_2 (NT) and (B) S-TiO_2 (ST) recorded at 77K

The trapped electrons and holes is as given below.

$$h^+ + OH^- \longrightarrow {}^{\cdot}OH \quad (1)$$

$$2\ {}^{\cdot}OH \longrightarrow H_2O_2 \quad (2)$$

$$H_2O_2 + h^+ \longrightarrow O_2^- + 2H^+ \quad (3)$$

$$O_2^- + h^+ \longrightarrow O_2 \quad (4)$$

As the samples were prepared at low temperature and less percentage of N and S doping sources in TiO_2, $N^{\cdot}$-hole signal was not observed in N-TiO_2. This infers that N and sulfur were on the surface but not inside the lattice.

3.2. Photocatalytic degradation of HD

Photocatalytic activity of ST nanocatalyst was examined by monitoring the degradation of HD in the presence sunlight irradiation. There was no obvious change of concentration of HD under the sole treatment of sunlight even after 6-8 h of irradiation. It is evident that, photodegradation of HD under the sole treatment of sunlight is not a significant process as it could not absorb sunlight above 290 nm . Further, there was no significant loss of HD due to evaporation or degradation owing to heat produced by sunlight. In the absence of light and in the presence of catalyst, 40 to 50 % of HD was observed to be degraded in 8 h on all the nanocatalysts. The degradation reactions were found to be very slow, incomplete, and led only to hydrolysis products like hemisulfur mustard and thiodiglycol as per GC-MS data. The degradation of HD in the absence of sunlight could be ascribed to available surface area, surface hydroxyl groups, Lewis acid sites, and the moisture present on the surface (1-3 % w/w) of the catalyst.

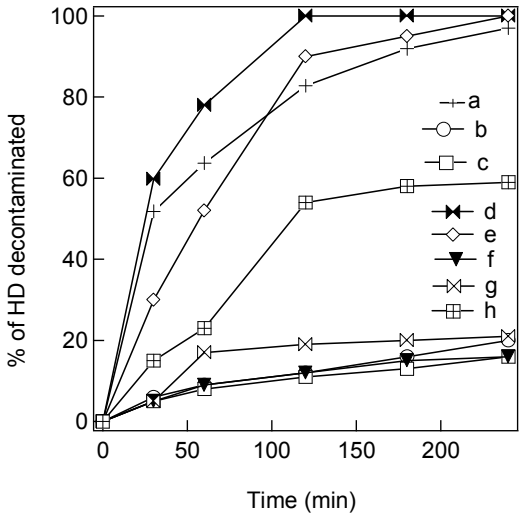

Fig. 7. HD degradation reactions on CT, HT, NT, and ST nanocatalysts in presence of sunlight and in the absence of light; a) NT + sunlight b) NT+ dark c) ST+ dark d) ST+ sunlight e) HT + sunlight f) HT + Dark g) CT + dark h) CT + sunlight .

ST nanocatalyst showed greater activity towards the photocatalytic degradation of HD when compared with NT or HT or CT nanocatalysts. It could be seen that NT and ST nanocatalysts showed much higher photocatalytic activities under sunlight than HT nanocatalyst. Under sunlight irradiation, ST nanocatalyst, NT nanocatalyst, and undoped nano TiO_2 degraded 100 % of HD in 120 min, 180 min, 240 min respectively. CT nanocatalyst took 420 min for 100 % degradation of HD as observed from Fig.7. Irrespective of catalyst, similar products were observed on doped (NT, ST) and undoped (HT, CT) nanocatalysts. On the whole, higher sunlight assisted photocatalytic degradation activity of S or N doped TiO_2 nanocatalyst could be attributed to the synergetic effects of strong absorption in the visible light region due to red shift of adsorption edge; and enhanced separation of charge carriers. Size of crystallites, large surface area of the S doped nano TiO_2 also facilitated this sunlight assisted photocatalytic degradation of HD. Relatively higher activity of ST nanocatalyst can be attributed to the highest absorption efficiency. The sulfur dopant was found to exist as either S^{4+} or S^{6+} (SO_4^{2-}) and substituted titanium ion as observed from XPS data. The dopant sites seemed to have facilitated enhanced trapping of electrons. The size difference of nitrogen and oxygen atoms is very less and hence the nitrogen dopants seemed to have occupied oxygen interstitial sites. This could also be a reason for enhanced activity of ST catalyst relative to NT nanocatalyst. ST and NT nanocatalysts were observed to be deactivated after 3rd use due to poisoning of nanocatalysts through formation of alkoxy species, H_2SO_4 and HCl on the surface of catalyst. Initially they exhibited 98, 100 % of HD degradation efficiency, then decreased to 95.0, 92.1 % when it was reused after washing with acetonitrile. However, it decreased to 85, 81.6 % after 3rd use and then to 65, 60 % after 5th use. On the other hand, ~ 95% of HD degradation was

observed continuously for fifth time when the titania was thoroughly washed with 30% hydrogen peroxide solution followed by washing with copious amount of water, ethanol and dichloromethane. It could be ascribed to regeneration of active sites poisoned due to formation of surface bound alkoxy species (1100 cm^{-1}) as well as sulfonate species (1126 cm^{-1}, 1200 cm^{-1}) and the conclusion is supported by IR data as previously reported [22].

Photocatalytic degradation of HD resulted in the formation of several products like HD sulfoxide, HD disulfide, chloro ethyl vinyl sulfide, chloro ethyl vinyl sulfoxide, bis (2-hydroxy ethyl sulphide) and other products like CH_3CHO, CO_2 and H_2O. GC-MS data was found to be similar to that which was already reported [22].

3.4. Mechanism of HD photocatalytic degradation

Sunlight is composed of 4-5% of UV light and 46 % of visible light [26]. It is apparent from data that, both UV and visible light fractions present in the sunlight contribute to photocatalytic degradation of HD. On non-metal doped nano TiO_2 (ST or NT), photogenerated holes and electrons are generated and quickly trapped on the surface defect sites on full light illumination. The trapped holes react with the HD molecule and degrade it directly. Superoxide anion radicals further react with moisture and form the hydroxyl radicals. These hydroxyl radicals react with HD and degrade it to the corresponding reaction products mentioned above. Formation of hydroxyl radicals on the surface of ST, NT, HT and CT in the presence of sunlight was probed by the reactions with DMSO. S or N doped TiO_2 nanoparticles were mixed with DMSO (1:1%, W/W) and exposed to sunlight . After exposure, products were extracted with ethanol, concentrated and subjected to GC–MS analysis. The GC–MS data indicated the formation of methane sulfonic acid ethyl ester and methane sulfonic acid as depicted by m/z values at 124, 109, 97, 79, 65, 45 and 96, 79, 65, 48, 31. Hydroxyl radical reacts with DMSO and converts it to methane sulfonic acid.

The reactions in absence of light lead to hydrolysis products. In presence of light, the decomposition of HD over titania systems leads to oxidation, elimination, rearranged products in addition to hydrolysis products. The products were consistent with earlier reports. GC-MS spectra of HD disulfide, HD sulfoxide, chloro ethyl vinyl sulfide, chloro ethyl vinyl sulfoxide were given in *SI*.

Decontamination of HD is also supported by FT-IR data as reported earlier. In the case of HD adsorbed on TiO_2, a band at 2930 cm^{-1} indicates C–H vibration of CH_2S, bands at around 1220 cm^{-1} and 1270 cm^{-1} correspond to CH_2 vibration of the CH_2–S group which are characteristics of adsorbed HD on nano TiO_2. Band at 700 cm^{-1} disappeared due to hydrolysis of HD on TiO_2 without irradiation. With irradiation of sunlight the band pattern observed to have changed. Weak band at around 1410 cm^{-1} indicates the formation of –COOH group typical of acetic acid formed during photocatalytic decontamination of HD on above said catalysts.

3. Experimental

3.1. Materials

Thiourea, urea, titanium tetraisopropoxide (TTIP), bis (trimethylsilyl) trifluoro acetamide were procured from Acros organics, UK. Dichloromethane, ethanol, ethyl acetate, hydrogen peroxide and acetonitrile were obtained from E. Merck India Ltd. HD of 99 % purity was obtained from synthetic chemistry division of our establishment (This is a very toxic agent; hence these experiments should be done under the guidance of trained personnel equipped with individual protective equipment only). Commercial nano TiO_2 (CT) was procured from Alfa Aeser, UK.

3.2. Preparation of nanocatalysts

TiO_2 nanocatalysts were prepared by sol-gel hydrolysis of titanium (IV) isopropoxide (TTIP) followed by hydrothermal treatment. TTIP was dissolved in anhydrous ethanol and the solution was added dropwise to the mixture of distilled water and ethanol under vigorous stirring at room temperature. Obtained gel was transferred into a Teflon lined autoclave and heated at 120˚C for 10 hrs. The resulted samples were centrifuged washed with water and ethanol and dried at 100˚C for 10h and finally labelled as undoped TiO_2 nanocatalyst (HT). N or S dopants were introduced by adding appropriate amounts of urea or thiourea into deionised water prior to the hydrolysis of TTIP. Obtained samples were labelled as NT (N/Ti=0.1) or ST (S/Ti =0.1) nanocatalyst.

3.3. Characterization of photocatalysts

XRD data was recorded on X'Pert Pro Diffractometer of Panalytical, Netherlands make using Cu Kα radiation.TEM measurements were done on Tecnai transmission electron microscope of FEI make. XPS data was recorded on KRATOS AXIS 165 instrument. Nitrogen adsorption measurements were done on ASAP 2020 surface area analyser of Micrometrics, USA. UV-visible absorption was obtained using Shimatzu UV-2500 spectrophotometer equipped with an integrating sphere. X-band Electron Paramagnetic Resonance (EPR) spectra were recorded by a Bruker EMX spectrometer. Gas chromatograph of Nucon Engineers, India make equipped with FID detector, BP5 column (30 m length, 0.5 mm i.d.) was used to monitor degradation of HD. GC–MS system (5975 B) of Agilent, USA make was used for quantification and identification of reaction products.

3.4. Photocatalytic degradation

100 mg of nanocatalyst (ST or NT or HT or CT) was taken in a quartz tube and 100 µL of dichloromethane solution containing 2 µL of HD was spiked on it and dichloromethane was allowed to evaporate. Subsequently, quartz tube containing the nano photocatalyst was irradiated with natural sunlight. Intensity of light was measured by digital light meter (SLM 110 model) of

A.W. Sperry Instruments, USA with help of adopters provided. Value of irradiance of sunlight was determined to be 95 mW/cm^2. All the experiments were carried out at 35±5˚ C. Remaining HD was extracted after periodic intervals of time using acetonitrile. The extracted samples were analyzed with GC affixed with FID detector to monitor the amount of degraded HD. Later, the solution was concentrated to 1 mL and analyzed for products by GC-MS. Few degradation products formed were identified by GC-MS (Model 5975B and 6890N). Reaction products like hemisulfur mustard & thiodiglycol were made GC amenable by silylation with bis trifluoro acetamide.

4. Conclusion

S-TiO_2 exhibited superior photocatalytic activity relative to N-TiO_2, undoped TiO_2 and commercial nano TiO_2 towards photocatalytic degradation under sunlight irradiation. This superior photocatalytic activity of doped nano TiO_2 materials relative to undoped nano TiO_2 can be attributed to the presence of S^{4+}/S^{6+} or N^- impurity levels. These impurity levels produce hydroxyl radicals by reducing the recombination rate towards the effective utilization of sunlight. The C-S bond cleavage, oxidation of S atom, hydrolysis, and elimination reactions seemed to have contributed to degradation of HD into non toxic products. These interesting properties make these materials as eco-friendly and potential sorbent for degradation of toxic chemicals.

Acknowledgements

Authors thank to the Director, DRDE, Gwalior for his permission to publish this work. They also thank Dr. Beer Singh, Head PD Division, DRDE, Gwalior, Prof. Ramesh Chandra, IITR, Prof. B. Sreedhar, IICT for providing GC-MS, TEM, XPS.

References

[a] *Department of Physics, National Dong Hwa University, Hualien, Taiwan 974-01*
E-mail: ramamsc2007@gmail.com ke@mail.ndhu.edu.tw
[b] *Defence Research & Development Establishment, Jhansi Road, Gwalior 474 002 (M.P.), India. E-mail: gkprasad2001@gmail.com*

1. A. Fujishima, K. Hashimto, T. Watanbe, TiO_2 Photocatalysis, Fundamentals and Applications, BKC Press, Tokyo, 1999, pp.1-160.
2. M.R. Hoffmann, S.T. Martin, W. Choi, D.W. Bahnemann, *Chem. Rev.*, 1995, **95**, 69.
3. M. Anpo, Catal. *Surv. Jpn*,. 1997, **1**, 169.
4. A.L. Linsebigler, G. Lu, J.T. Yates Jr., *Chem. Rev*., 1995, **95**, 735.
5. T.Umebayashi, T. Yamaki, H.Itoh, K.Asai, *Appl.Phys.Lett*., 2002, **81**, 454.
6. H. Irie, S. Washizuka, N. Yoshino, K. Hashimoto, *Chem. Commun.,* 2003, 1298.
7. H. Irie, Y. Watanabe, K. Hashimoto, *J. Phys. Chem. B.*, 2003, **107** 5483.
8. R. Asahi, T. Morikawa, T. Ohwaki, K. Aoki, Y. Taga, *Science.*, 2001, **293**, 269.
9. C. Burda, Y. Lou, X. Chen, A.C.S. Samia, J. Stout, J.L. Gole, Nano Lett., 2003, **3** , 1049.
10. T. Lindgren, J.M. Mwabora, E. Avendano, J. Jonsson, A. Hoel, C.G. Granqvist, S.E. Lindquist, *J. Phys. Chem. B*., 2003, **107**, 5709.
11. S. Sakthivel, H. Kisch, *ChemPhysChem.*, 2003, **4**, 487.
12. T. Ihara, M. Miyoshi, Y. Iriyama, O. Matsumoto, S. Sugihara, *Appl. Catal. B: Environ.*, 2003, **42**, 403.
13. S. Yin, Q. Zhang, F. Saito, T. Sato, *Chem. Lett.* , 2003, **32**. 358.
14. T. Umebayashi, T. Yamaki, H. Itoh, K. Asai, *Appl. Phys. Lett.*, 2002, **81**, 454.
15. T. Umebayashi, T. Yamaki, S. Tanala, K. Asai, *Chem. Lett.*, 2003, **32**, 330.
16. T. Umebayashi, T. Yamaki, S. Yamamoto, A. Miyashita, S. Tanala, T. Sumita, K. Asai, *J. Appl. Phys 2003,* **93**, 5156.
17. T. Ohno, T. Mitsui, M. Matsumura, *Chem. Lett.* , 2003, **32**, 364.
18. T. Ohno, M. Akiyoshi, T. Umebayashi, K. Asai, T. Mitsui, M. Matsumura, *Appl. Catal. A: General*., 2004, **265** , 115.
19. T. Ohno, *Water Sci. Technol*., 2004, **49** , 159.
20. W. Ho, J. Yu, S. Lee, *J. Solid State Chem.*, 2006, **179**, 1171.
21. M. L. Hitchman, R. A. Spackman, F. J. Yusta, B. Morel, *Sci. Global Secur*., 1997, **6**, 205.
22. a) P.V.R.K. Ramacharyulu, G.K.Prasad, K. Ganesan, Beer Singh, *J. Mol. Catal. A: Chem.*, 2012, **353** , 132. b) G.K.Prasad, P.V.R.K. Ramacharyulu, B. Singh, K. Batra, A. R. Srivastava, K. Ganesan, R. Vijayaraghavan, *J Mol Cat A.Chem,* 2011, **349(1-2)**, 55. c) P.V.R.K. Ramacharyulu, J Praveen Kumar, G.K.Prasad, B.Singh, K.Ganesan, K. Dwivedi, *Environ. prog. & Sustain. Ener.*, 2013, **32** , 1118. d) P.V.R.K. Ramacharyulu, G.K.Prasad, J Praveen Kumar, B. Singh, K.Ganesan, K. Dwivedi, *J. Mol. Catal. A: Chem.*, 2014, **387** , 38.
23. B. Cojocaru, S.Neatu, V.I.Parvulescu, V.Somoghi, N.Petrea, G.E.Pure, M.Alvaro, H.Garcia, *ChemSusChem*., 2009, **2**, 427.
24. G.yang, Z.Yan, T. Xiao, *Appl. Surf. Sci.,* 2012, 258, 4016.
25. C.P. Kumar,N.O. Gopal, T.C. Wang, M.S. Wong, S.C.Ke, *J. Phys. Chem. B*, 2006, **110**, 5223.
26. T. Bak, J. Nowotny, M. Rekas, C.C. Sorrell, *Int. J. Hydrogen Energy.*, 2002, **27**, 991.

